

A PHOTOEVAPORATING ROTATING DISK IN THE CEPHEUS A HW2 STAR CLUSTER.

I. JIMÉNEZ-SERRA¹, J. MARTÍN-PINTADO¹, A. RODRÍGUEZ-FRANCO^{1,2}, C. CHANDLER³, C. COMITO⁴ AND P. SCHILKE⁴
Draft version October 28, 2018

ABSTRACT

We present VLA and PdBI subarcsecond images ($\sim 0.15''$ - $0.6''$) of the radiocontinuum emission at 7 mm and of the SO₂ $J = 19_{2,18} \rightarrow 18_{3,15}$ and $J = 27_{8,20} \rightarrow 28_{7,21}$ lines toward the Cepheus A HW2 region. The SO₂ images reveal the presence of a hot core internally heated by an intermediate mass protostar, and a circumstellar rotating disk around the HW2 radio jet with size 600 AU \times 100 AU and mass of $\sim 1 M_{\odot}$. Keplerian rotation for the disk velocity gradient of $\sim 5 \text{ km s}^{-1}$ requires a $9 M_{\odot}$ central star, which cannot explain the total luminosity observed in the region. This may indicate that the disk does not rotate with a Keplerian law due to the extreme youth of this object. Our high sensitivity radiocontinuum image at 7 mm shows in addition to the ionized jet, an extended emission to the west (and marginally to the south) of the HW2 jet, filling the south-west cavity of the HW2 disk. From the morphology and location of this free-free continuum emission at centimeter and millimeter wavelengths (spectral index of ~ 0.4 - 1.5), we propose that the disk is photoevaporating due to the UV radiation from the central star. All this indicates that the Cepheus A HW2 region harbors a cluster of massive stars. Disk accretion seems to be the most plausible way to form massive stars in moderate density/luminosity clusters.

Subject headings: stars: formation — ISM: individual (Cepheus A) — ISM: molecules

1. INTRODUCTION

Massive stars (in excess of $\sim 8 M_{\odot}$) are known to form in clusters within the dense cores of giant molecular clouds (Garay & Lizano 1999). The formation processes of these stars, however, still remain unclear. It has been proposed that massive stars form either through accretion of material from a circumstellar disk (McKee & Tan 2003) or through the merging of several low mass stars (Bonnell & Bate 2002). Since the sites of massive star formation are located at distances of ≥ 0.5 kpc, subarcsecond observations are therefore required to measure small scale structures relevant to the star formation process.

Cepheus A East (at 725 pc; Johnson 1957) is a very active region of massive star formation (see e.g. Hughes & Wouterloot 1984; Torrelles et al. 1996; Garay et al. 1996; Gómez et al. 1999). The HW2 radio jet, the brightest radio source in the region (Hughes & Wouterloot 1984), is known to power the large-scale molecular outflow seen in the northeast-southwest direction (Narayanan & Walker 1996; Gómez et al. 1999). Perpendicular to the jet-outflow axis, Torrelles et al. (1996) inferred the presence of a rotating and contracting circumstellar disk (size of $0.8''$, i.e., 600 AU) from the spatial and velocity distribution of the water maser emission around the HW2 jet.

Patel et al. (2005) have recently reported a flattened CH₃CN structure (beam of $\sim 1''$) with size

$1.6''$ (~ 1200 AU) suggesting that all molecular emission around HW2 is located in a rotating disk. However, the detection of the first hot core associated with an intermediate mass protostar in the vicinity of HW2 (Martín-Pintado et al. 2005) clearly contrasts with the idea of a single protostellar source undergoing disk accretion as suggested by Patel et al. (2005). Furthermore, linear/arcuate water maser structures (Torrelles et al. 2001) and high angular resolution radio continuum observations (Curiel et al. 2002), have revealed, at least, three different young stellar objects (YSOs) within a projected area of $\sim 0.6'' \times 0.6''$, making the actual picture of the Cepheus A HW2 region even more complex.

The morphology of the ionized gas restricted to the radio jet in all directions, however, requires the presence of circumstellar material confining the UV photons emitted by the exciting source. In this Letter, we present subarcsecond ($\sim 0.15''$ - $0.6''$) VLA and PdBI images which resolve for the first time the hot molecular gas around HW2 in a photoevaporating rotating disk around the radio jet and a nearby hot core. The hot core is an independent protostar in the cluster around HW2 that likely drives the east-west outflow found in the region.

2. OBSERVATIONS & RESULTS

The observations of the SO₂ $J = 19_{2,18} \rightarrow 18_{3,15}$ ($E_u = 183$ K) line toward the Cepheus A HW2 region were carried out in 2005 April 12 with the Very Large Array (VLA) in the B configuration. We used the 2IF (AD) spectral line mode with a bandwidth of 12.5 MHz and 32 channels per IF. The spectral resolution provided by the correlator was of 390.625 kHz ($\sim 2.7 \text{ km s}^{-1}$ at 7 mm). The central channel was set at -10 km s^{-1} (Martín-Pintado et al. 2005). 3C84 (~ 9.00 Jy), 3C48 (~ 0.64 Jy) and 2250+558 (~ 0.46 Jy) were used as band-pass, flux density and phase calibrators, respectively. Calibration, continuum subtraction, (natural weighted) imaging and cleaning were carried out with AIPS. The

¹ Departamento de Astrofísica Molecular e Infrarroja, Instituto de Estructura de la Materia (CSIC), C/ Serrano 121, E-28006 Madrid; izaskun@damir.iem.csic.es, martin@damir.iem.csic.es, arturo@damir.iem.csic.es

² Escuela Universitaria de Óptica, Departamento de Matemática Aplicada (Biomatemática), Universidad Complutense de Madrid, Avda. Arcos de Jalón s/n, E-28037 Madrid, Spain

³ National Radio Astronomy Observatory P.O. Box O Socorro NM 87801; cchandle@aoc.nrao.edu

⁴ Max Planck Institute for Radio Astronomy Auf dem Hügel 69 D-53121 Bonn; ccomito@mpifr-bonn.mpg.de, schilke@mpifr-bonn.mpg.de

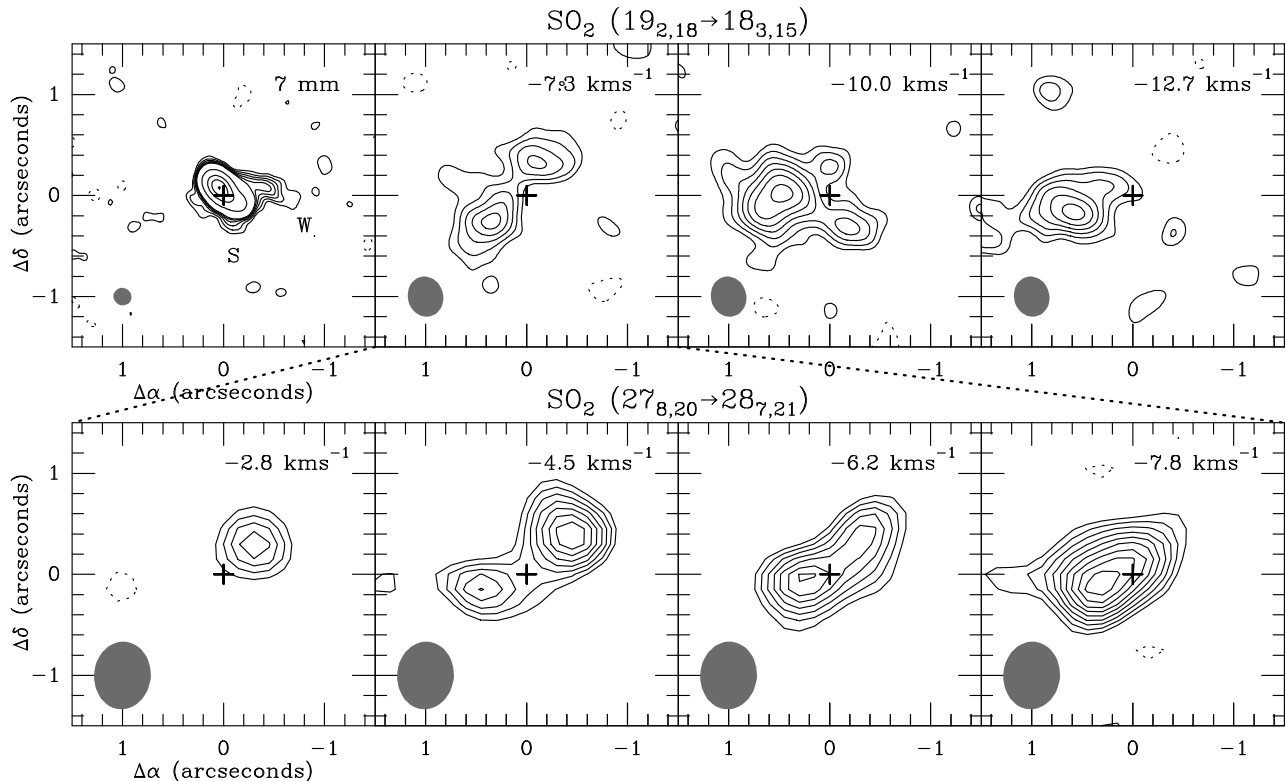


FIG. 1.— Upper panels: Radio continuum emission at 7 mm and SO_2 $J=192_{18}\rightarrow 183_{15}$ line images observed at -7.3 , -10.0 and -12.7 km s^{-1} with the VLA. The contour levels for the continuum map are -0.4 , 0.4 (2σ), 0.6 , 0.8 , 1.0 , 1.2 , 1.4 , 5 , 13 , 21 and 29 mJy beam^{-1} , and for the SO_2 images are -3 , 2 (2σ), 3 , 4 , 5 , 6 , 7 and 8 $\text{mJy beam}^{-1} \text{ km s}^{-1}$. Lower panels: SO_2 $J=278_{20}\rightarrow 287_{21}$ line maps at -2.8 , -4.5 , -6.2 and -7.8 km s^{-1} observed with the PdBI. The contour levels are -3 , 3 , 4 , 5 , 6 , 7 , 8 and 9×14 $\text{mJy beam}^{-1} \text{ km s}^{-1}$, the 1σ noise level of the maps. Beam sizes are shown at lower left corner and the reference position is $[\alpha(J2000) = 22^{\text{h}}56^{\text{m}}17.98^{\text{s}}$, $\delta(J2000) = +62^{\circ}01'49.5''$].

SO_2 $J = 278_{20}\rightarrow 287_{21}$ ($E_u=505$ K) line was observed between 2003 December and 2004 March with the IRAM Plateau de Bure Interferometer (PdBI) in the AB configuration. The final maps are 1.6 km s^{-1} channel width. We used 3C454.3 (~ 7 Jy), NRAO150 (~ 3 Jy) and 2037+511 (~ 0.6 Jy) as band-pass, flux density and phase calibrators respectively. Calibration, continuum subtraction, imaging and cleaning were done with GILDAS.

In Fig. 1 (upper panels), we show the 7 mm continuum map (beam of $0.18'' \times 0.16''$, P.A. = 30°) obtained by averaging line-free channels, and the SO_2 $J = 192_{18}\rightarrow 183_{15}$ line images at -7.3 , -10.0 and -12.7 km s^{-1} (beam of $\sim 0.35''$) obtained by tapering our data with a Gaussian function of $500 \text{ k}\lambda$. We resolve the continuum emission in the strong thermal radio jet (deconvolved size of $0.3'' \times 0.1''$), and a weak extended structure to the west, and marginally to the south, of HW2 (hereafter, the W and S components; see Fig. 1). The orientation of the radio jet (P.A. $\simeq 46^\circ$) is similar to that derived by Rodríguez et al. (1994). The peak continuum intensity is $27.8 \pm 0.2 \text{ mJy}$ and the integrated flux of the radio jet is $\sim 53 \text{ mJy}$, in agreement with the results of Curiel et al. (2006). The W component is detected at a 8σ level with a peak intensity of 1.2 mJy . This continuum emission is also barely observed at 3.6 cm (epochs 2000 and 2002; see Curiel et al. 2006) at a 2σ level. The lack of detection of the W component in the 1.3 cm maps of Curiel et al. (2006) is consistent with a spectral index of ~ 1.5 (Sec. 3). Despite the smaller spatial extension of the S component,

this emission could be the counterpart of the VLA-R5 source seen at 3.6 cm (Curiel et al. 2002, 2006).

The SO_2 $J = 192_{18}\rightarrow 183_{15}$ emission of Fig. 1 (upper panels) reveals different features in the vicinity of the HW2 radio jet. The -7.3 km s^{-1} channel map (integrated flux of 38 mJy) shows an elongated structure with an orientation (P.A. $\simeq -34^\circ$) nearly perpendicular to that of the radio jet and reminiscent of a disk. Images of the emission from several molecules show a chemical segregation of the hot cores around HW2 (Comito et al. 2007; Brogan et al. 2007), with the SO_2 emission peaking toward the east of HW2. Our SO_2 images, however, show that this molecule is clearly sampling a coherent spatial structure at both sides of the radio jet as expected for a circumstellar disk around HW2. Furthermore, the higher sensitivity and velocity resolution PdBI images of the SO_2 $J = 278_{20}\rightarrow 287_{21}$ line (lower panels in Fig. 1), show that the redshifted emission at -2.8 km s^{-1} is located to the northwest of HW2 while the blueshifted emission at -7.8 km s^{-1} is located to the southeast of the radio jet. This velocity gradient of $\sim 5 \text{ km s}^{-1}$ is consistent with a rotating disk. Although the central velocity of the disk ($\sim -5 \text{ km s}^{-1}$) is different from the systemic velocity of the cloud ($\sim -10 \text{ km s}^{-1}$), it is not uncommon to find protostars with velocities different from that of the ambient cloud (e.g. Morris, Palmer & Zuckerman 1980).

All the morphological and kinematical evidences therefore point toward a circumstellar rotating disk around HW2 with a deconvolved size of $0.8'' \times 0.15''$

(600 AU \times 100 AU). This size is much smaller than that obtained by Patel et al. (2005), and consistent with the disk size inferred by Torrelles et al. (1996). Although we cannot rule out the possibility that any substantial flaring could appear at smaller scales than our beam, the circumstellar disk around HW2 seems to be very thin.

The SO₂ $J=19_{2,18} \rightarrow 18_{3,15}$ channel map at -10.0 km s⁻¹ (Fig. 1) shows a compact condensation (size of $0.6''$ and integrated flux of 50 mJy) whose location ($\sim 0.4''$ east of HW2) coincides with that of the hot core heated by an intermediate mass protostar reported by Martín-Pintado et al. (2005). For the -12.7 km s⁻¹ channel (Fig. 1), we find elongated SO₂ emission in the southeast-northwest direction (size of $\sim 0.7'' \times 0.4''$, P.A. = -72° , and integrated flux of 35 mJy) whose emission peak is located $\sim 0.7''$ (500 AU) east of HW2, suggesting that this emission is not associated with the hot core.

3. THE DISK AROUND THE HW2 RADIO JET

Fig. 2 shows the superposition of the SO₂ $J=19_{2,18} \rightarrow 18_{3,15}$ -7.3 km s⁻¹ channel map (thin contours and grey scale) on the radiocontinuum images (thick solid contours) at 7 mm (upper panel) and 3.6 cm (lower panel; Curiel et al. 2006). The morphology of the SO₂ emission shows that the circumstellar molecular disk confines the HW2 radio jet. The location of the central source (see filled stars in Fig. 2; Curiel et al. 2006) is very close to the geometrical center of the disk and to the peak of the continuum emission at 7 mm.

The water vapor masers reported by Torrelles et al. (1996) are distributed along the SO₂ emission (Fig. 2), supporting the idea of a rotating disk around the HW2 ionized jet. Since the H₂O maser emission is located at the interface between the radio jet and the HW2 disk, the kinematics of the water masers are likely dominated by the jet-disk interaction. In particular, the R4 arcuate maser structure (Torrelles et al. 2001) traces the edge of the disk as if the masers were located on its surface. The R1, R2 and R3 linear maser structures delineate the north-west edge of the radio jet, suggesting that the ionized jet is generating a cavity as it propagates through the molecular gas (Torrelles et al. 2001). The submillimeter water masers tracing the hot gas (Patel et al. 2007), appear at the inner region of the disk.

Fig. 2 also shows that the W and S continuum features clearly fill and surround the south-west cavity of the HW2 disk. By comparing our 7 mm continuum image with that of Curiel et al. (2006) at 3.6 cm (Fig. 2), we estimate the spectral index, α ($S_\nu \propto \nu^\alpha$), of the W and S components. Using the 3.6 cm peak flux of Fig. 2, we derive a spectral index of 1.5 for the W component. From the 3σ level noise of our 7 mm map, an upper limit for the spectral index of ≤ 0.4 is also derived for the VLA-R5 continuum source, consistent with that previously obtained by Curiel et al. (2002). As discussed in Sec. 5, this free-free continuum emission may be explained by the photoevaporation of the HW2 disk by the UV radiation of the central source.

We can make a rough estimate of the mass of the disk by considering the integrated SO₂ emission measured at -7.3 km s⁻¹. Assuming an excitation temperature of ~ 160 K (see below and Martín-Pintado et al. 2005), the SO₂ column density within the disk,

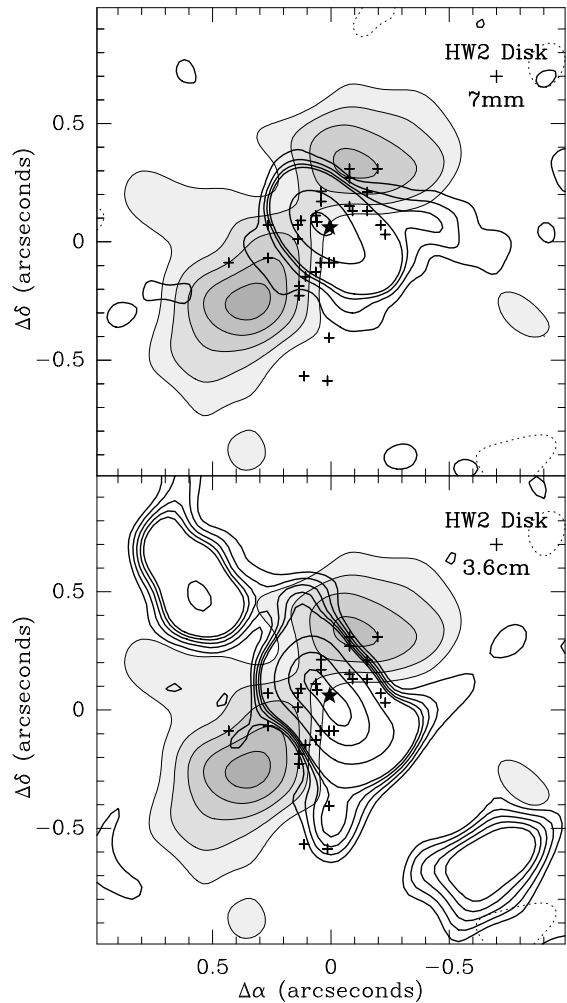


FIG. 2.— SO₂ emission map at -7.3 km s⁻¹ (thin contours and grey scale) superimposed on our 7 mm continuum image (thick contours, upper panel) and on the 3.6 cm continuum map of Curiel et al. (2006) for the 2000 epoch (thick contours, lower panel). Contour levels for the 7 mm map are -0.4 , 0.4 (2σ), 0.8 , 1.2 , 1.6 , 10 and 26 mJy beam⁻¹, and for the 3.6 cm image are 0.08 (2σ), 0.12 , 0.16 , 0.20 , 0.24 , 0.64 , 1.28 and 1.92 mJy beam⁻¹. Contour levels for the SO₂ emission are as in Fig. 1. Crosses mark the positions of the water masers (Torrelles et al. 1996). Filled stars show the location of the powering source of the HW2 jet (Curiel et al. 2006).

given by $N(\text{SO}_2) = 1.4 \times 10^7 \frac{\nu(\text{GHz})^2}{A_{ul} g_u} \int T_B dv$ (K km s⁻¹), is $\sim 6 \times 10^{18}$ cm⁻². If we now consider an edge-on disk with a radius of $R=300$ AU and a height of $h=100$ AU, the disk mass can be estimated as $M_d = 6 \times 10^{-31} R(\text{AU}) h(\text{AU}) N(\text{SO}_2) \chi(\text{SO}_2)^{-1} M_\odot$. For a SO₂ abundance of $\sim 10^{-7}$ (Charnley 1997), the disk mass would be $\sim 1 M_\odot$. Also, assuming Keplerian rotation for the velocity gradient of the disk [$\Delta v \sim 5$ km s⁻¹ and $M_* = 1.25 \times 10^{-3} (\frac{\Delta v}{\text{km s}^{-1}})^2 (\frac{R}{\text{AU}}) M_\odot$], we derive a binding mass of the central source of $M_* \sim 9 M_\odot$ (B2 type star), which is a factor of 2 smaller than that obtained by Patel et al. (2005).

4. HOT CORE AND SHOCKED OUTFLOWING GAS

The SO₂ $J=19_{2,18} \rightarrow 18_{3,15}$ emission at -10 km s⁻¹ (Fig. 1) resolves the hot core located $0.4''$ east of the HW2 jet. From the line peak flux at -10 km s⁻¹, and

using the size of $\sim 0.6''$ and a linewidth of $\sim 5 \text{ km s}^{-1}$ (Martín-Pintado et al. 2005), we find that the upper level SO_2 column density averaged in a beam of $24''$ is $N_u/g_u \sim 2 \times 10^{11} \text{ cm}^{-2}$. This SO_2 column density is fully in agreement with an excitation temperature of $\sim 160 \text{ K}$ (see the SO_2 population diagram in Martín-Pintado et al. 2005), as expected if this emission traced the hot core associated with an intermediate mass protostar.

The -12.7 km s^{-1} SO_2 emission (Fig. 1) is located $0.3''$ east from the hot core. As discussed in Sec. 5, this displacement, plus the spatially extended morphology and orientation of this emission, suggest a close association with shocked gas of one of the outflows in the region.

5. DISCUSSION

The subarcsecond VLA and PdBI images of the high-J SO_2 lines have revealed the presence of a hot core heated by a YSO and a rotating disk around the HW2 jet. Furthermore, the 7 mm and 3.6 cm radiocontinuum images show free-free emission at the south-west cavity of the disk suggesting that it is photoevaporating (Hollenbach et al. 1994). The derived spectral index of this emission ($\alpha \sim 0.4-1.5$) is similar to those obtained by Jaffe & Martín-Pintado (1999) for the broad recombination line objects that were proposed to be associated with photoevaporating disks. Most of these objects are very distant, making it difficult to resolve the neutral disk and the ionized flow produced by the photoevaporation. So far, only MWC 349 has been studied in some detail from recombination line masers (Martín-Pintado 2002). However, MWC 349 is a rather evolved object which does not show the highly collimated jet but only the low velocity outflow. If confirmed, the HW2 system would offer an unique opportunity to study the early phase of the ionized flow generated by photoevaporation of disks.

Our estimate for the mass of the disk ($\sim 1 M_\odot$) is consistent with that obtained by Patel et al. (2005). This high disk mass could a priori contrast with those derived for early B-type stars ($\sim 0.2 M_\odot$; Natta, Grinin & Mannings 2000). However, since disk material is rapidly dispersed by photoevaporation in Herbig Be stars (Fuente et al. 2001), the detection of a massive disk around HW2 is in agreement with an object being at an early stage of its evolution.

For the central source, however, we note that a B2 type star as inferred from the Keplerian rotation, will provide a luminosity of $\sim 5 \times 10^3 L_\odot$ which is only 25% the total IR luminosity measured in the Cepheus A HW2 region, believed to be dominated by the HW2 powering source ($\sim 2 \times 10^4 L_\odot$; Evans et al. 1981). Furthermore, the rate of ionizing photons derived for the central star

is consistent with a B0.5 star with $\sim 20 M_\odot$. Recent non-Keplerian disk models show that small deviations from the Keplerian rotation in a disk at the early stages of its formation, properly fit the molecular and continuum emission observed in low mass stars, avoiding the underestimation of the central source mass due to the Keplerian law assumption (Piétu, Guilloteau, & Dutrey 2005). Non-Keplerian rotation could be the explanation of the relatively small mass derived for the powering source of the HW2 jet.

Our images show that the hot core is an independent object located in the vicinity of HW2. In addition to the hot core, we have also detected low velocity (blue-shifted) SO_2 emission $0.3''$ east of the hot core. High angular interferometric SiO images have shown low velocity gas (red- and blue-shifted) in the surroundings of the hot core along the southeast-northwest direction (Comito et al. 2007). In particular, the location of the low velocity SO_2 emission coincides with the blue-lobe of the small-scale SiO outflow (Comito et al. 2007), supporting the idea that this SO_2 emission is shocked gas associated with the east-west outflow seen in CO (Narayanan & Walker 1996) and likely driven by the protostar associated with the hot core.

The detection of a circumstellar disk around the HW2 radio jet in a cluster of massive stars favors the hypothesis of accretion of material through a circumstellar disk for the formation of these objects (McKee & Tan 2003). This is expected since the Cepheus A HW2 region is a relatively low density cluster. However, in high density clusters, it may not be unlikely that massive stars form through the coalescence of low mass stars as proposed by Bonnell & Bate (2002).

In summary, our subarcsecond images have resolved for the first time the hot gas surrounding the Cepheus A HW2 massive star cluster. A rotating disk of radius 300 AU and a mass of $1 M_\odot$ is photoevaporating by the central UV photons of the powering source of the HW2 radio jet. Our VLA images also resolve the nearby hot core associated with an intermediate mass star. This object is independent from the central source of the HW2 jet, and powers the east-west outflow found in the region. The formation of the most massive star in moderate luminosity clusters may be produced through accretion disks.

We thank S. Curiel for kindly providing the radiocontinuum image at 3.6 cm in Fig. 2. We also acknowledge the Spanish MEC for the support provided through projects number ESP2004-00665, AYA2003-02785-E and ‘‘Comunidad de Madrid’’ Government under PRICIT project S-0505/ESP-0277 (ASTROCAM).

REFERENCES

- Bonnell, I. A., & Bate, M. R. 2002, MNRAS, 336, 659
 Brogan, C. L., Chandler, C. J., Hunter, T. R., Shirley, Y. L., & Sarma, A. P. 2007, ApJ, submitted
 Charnley, S. B. 1997, ApJ, 481, 396
 Comito, C., Schilke, P., Endesfelder, U., Jiménez-Serra, I., & Martín-Pintado, J. 2007, A&A, submitted
 Curiel, S., et al. 2002, ApJ, 564, L35
 Curiel, S., et al. 2006, ApJ, 638, 878
 Evans, N. J., II, et al. 1981, ApJ, 244, 115
 Fuente, A., Neri, R., Martín-Pintado, J., Bachiller, R., Rodríguez-Franco, A., & Palla, F. 2001, A&A, 366, 873
 Garay, G., Ramírez, S., Rodríguez, L. F., Curiel, S., & Torrelles, J. M. 1996, ApJ, 459, 193
 Garay, G., & Lizano, S. 1999, PASP, 111, 1049
 Gómez, J. F., Sargent, A. I., Torrelles, J. M., Ho, P. T. P., Rodríguez, L. F., Cantó, J., & Garay, G. 1999, ApJ, 514, 287
 Hollenbach, D., Johnstone, D., Lizano, S., & Shu, F. 1994, ApJ, 428, 654
 Hughes, V. A., & Wouterloot, J. G. A. 1984, ApJ, 276, 204
 Jaffe, D. T., & Martín-Pintado, J. 1999, ApJ, 520, 162
 Johnson, H. L. 1957, ApJ, 126, 121

- Martín-Pintado, J. 2002, in 206 IAU Symposium: Cosmic Masers. From Proto-Stars to Black Holes, Ed. V. Mineese & M. Reid. San Francisco: Astronomical Society of the Pacific, p. 226
- Martín-Pintado, J., Jiménez-Serra, I., Rodríguez-Franco, A., Martín, S., & Thum, C. 2005, *ApJ*, 628, L61
- McKee, C., & Tan, J. 2003, *ApJ*, 585, 850
- Morris, M., Palmer, P., & Zuckerman, B. 1980, *ApJ*, 237, 1
- Narayanan, G., & Walker, C. K. 1996, *ApJ*, 466, 844
- Natta, A., Grinin, V. P., & Mannings, V. 2000, in *Protostars and Planets IV*, ed. V. Mannings, A. Boss, & S. S. Russell (Tucson: University of Arizona Press), 559
- Patel, N. A., et al. 2005, *Nature*, 437, 109
- Patel, N. A., Curiel, S., Zhang, Q., Sridharan, T. K., Ho, P. T. P., & Torrelles, J. M. 2007, *ApJ*, in press
- Piétu, V., Guilloteau, S., & Dutrey, A. 2005, *A&A*, 443, 945
- Rodríguez, L. F., Garay, G., Curiel, S., Ramírez, S., Torrelles, J. M., Gómez, Y., & Velázquez, A. 1994, *ApJ*, 430, L65
- Torrelles, J. M., Gómez, J. F., Rodríguez, L. F., Curiel, S., Ho, P. T. P., Garay, G. 1996, *ApJ*, 457, L107
- Torrelles, J. M., Gómez, J. F., Garay, G., Rodríguez, L. F., Miranda, L. F., & Curiel, S. 1999, *MNRAS*, 307, 58
- Torrelles, J. M., et al. 2001, *ApJ*, 560, 853